Published in final edited form as:
J Immunol. 2008 July 15; 181(2): 1499–1506.

Chemotactic activity of S100A7 (psoriasin) is mediated by RAGE and potentiates inflammation with highly homologous but functionally distinct S100A15

Ronald Wolf[1], **O.M. Zack Howard**[2], **Hui-Fang Dong**[3], **Christopher Voscopoulos**[1], **Karen Boeshans**[4], **Jason Winston**[1], **Rao Divi**[1], **Michele Gunsior**[5], **Paul Goldsmith**[5], **Bijan Ahvazi**[4], **Triantafyllos Chavakis**[6], **Joost J Oppenheim**[2], and **Stuart H. Yuspa**[1]

1*Laboratory of Cancer Biology and Genetics, Center for Cancer Research, National Cancer Institute, Bethesda, MD*

2*Laboratory of Molecular Immunoregulation, Cancer and Inflammation Program, Center for Cancer Research, National Cancer Institute-Frederick, MD*

3*SAIC Frederick, Division of Basic Sciences and Cellular Immunology, National Cancer Institute-Frederick, MD*

4*X-ray Crystallography Facility, NIAMS, National Institutes of Health, Bethesda, MD*

5*Antibody and Protein Purification Unit, Center for Cancer Research, National Cancer Institute, Bethesda, MD*

6*Experimental Immunology Branch, Center for Cancer Research, National Cancer Institute, Bethesda, MD*

Abstract

Human S100A7 (psoriasin) is overexpressed in inflammatory diseases. The recently discovered, co-evolved hS100A15 is almost identical in sequence and upregulated with hS100A7 during cutaneus inflammation. The functional role of these closely related proteins for inflammation remains undefined. By generating specific antibodies, we demonstrate that hS100A7 and hS100A15 proteins are differentially expressed by specific cell types in the skin. Although highly homologous, both proteins are chemoattractants with distinct chemotactic activity for leukocyte subsets. We define RAGE (receptor of advanced glycated end products) as the hS100A7 receptor, whereas hS100A15 functions through a Gi protein coupled receptor. hS100A7-RAGE binding, signaling and chemotaxis are zinc-dependent in vitro, reflecting the previously reported zinc-mediated changes in the hS100A7 dimer structure. When combined, hS100A7 and hS100A15 potentiate inflammation in vivo. Thus, proinflammatory synergism in disease may be driven by the diverse biology of these almost identical proteins that have just recently evolved. The identified S100A7 interaction with RAGE may provide a novel therapeutic target for inflammation.

Keywords

neutrophils; cytokine; cytokine receptor; chemotaxis; inflammation

Correspondence to: Stuart H. Yuspa, MD, Laboratory of Cancer Biology and Genetics, Center for Cancer Research, National Cancer Institute, National Institutes of Health, 37 Convent Drive, MSC-4255, Building 37, Room 4068A, Bethesda, MD 20892-4255, Phone: (301) 496-2162, Fax: (301) 496-8709, email: yuspas@mail.nih.gov.

Introduction

Human S100A7 (hS100A7, psoriasin) was first identified as a protein upregulated in inflamed hyperplastic psoriatic skin 1. Since then, human S100A7 (hS100A7) has been widely studied because it is differentially expressed and released during inflammation 2–5. Recently, hS100A15, highly homologous to hS100A7, was also identified as upregulated in psoriasis, thereby suggesting a role in the inflammatory phenotype 6. However, the characteristics and functional mechanisms that link both hS100A7 and hS100A15 to inflammation are not defined. Both proteins belong to the multigenic S100 family of EF-hand proteins[7;8]. Despite their small size and conserved functional domains, gene duplications and variations throughout vertebrate evolution led to an increase in number and diversity within the S100 family. Genomic analysis of the hS100A7 and hS100A15 encoding chromosomal regions (Chromosome 1q21, Epidermal Differentiation Complex) reveals that both evolved recently by gene duplications during primate evolution, diverging the least among all S100 family members [9;10]. Thus, their high homology (93% sequence identity) makes it difficult to distinguish them when co-expressed. To address this further, we have developed unique reagents and functional assays to dissect similarities and differences among these closely related homologs. This study provides insight into properties and functional mechanism of S100A7 and S100A15 induced inflammation and reveals an unexpected biological diversity that may drive their functional synergism in inflammatory diseases.

Material and Methods

All the materials and methods used have been approved by the NCI.

Cloning, protein expression and purification

cDNA was prepared by PCR-cloning of full-length transcripts (hS100A7: NM_002963; hS100A15: AY189119) isolated from human skin 6. Proteins were expressed in *Escherichia coli BL21* (DE3) cells harboring plasmid his6-MBP-tev-human S100A15/– human S100A7, and proteins were purified as described 11. Purified S100 protein, a single band on Coomassie-stained gels (Mr ~ 12 kDa) was purged of endotoxin prior to experiments by chromatography onto Detoxigel columns (Pierce, Arlington Heights, IL) with endotoxin levels < 0.05 EU/μg protein. Endotoxin levels are below biological activity as demonstrated in-vivo and in-vitro inflammation and chemotaxis assays demonstrating that neutralization of S100 proteins or heating abrogated functional activity.

Cell culture

Normal human keratinocytes (Cascade Biologics, Portland, OR) were cultured in keratinocyte growth medium containing insulin (5 μg/mL) and bovine pituitary extract (50 μg/ml) at 37 °C in air containing 5% CO_2. Keratinocytes washed twice with PBS were harvested into lysis buffer for protein analysis (Cell Signaling, Beverly, MA) as described below. CHO cells were cultured in HAM's F12 (Invitrogen, Carlsbad, CA) with 10% BSA plus Zeocin (200 μg/mL) for selection of RAGE transfectants at 37 °C in air containing 5% CO_2 12.

Establishment of antibodies specific for hS100A7 and hS100A15, *in vitro* stimulation assay, immunoblot analysis, immunofluorescent staining

Monospecific antisera to human S100A15 were prepared in rabbits by injecting a synthetic peptide which corresponds to the N-terminal amino acid sequence of the deduced hS100A15 protein (gene bank acc. number AAO40032). The antibodies were affinity purified using the synthetic peptide-coupled to Affigel-15 (Biorad, St. Louis, MS). Most of the commercial and donated hS100A7 antibodies tested detected both proteins (data not shown). The monoclonal anti-hS100A7 antibody (Imgenex, San Diego, CA; Abcam, Cambridge, MA) specifically

detects recombinant S100A7 monomer without crossreacting with recombinant hS100A15 or several other hS100 proteins (50 ng/lane) (Fig. 1A). hS100A8 and hS100A10 (Novus Biologicals, Littleton, CO) were used as controls. In addition, pre-adsorptions with increasing doses of the corresponding cognate proteins blocked respective S100 antibody staining (13 and data not shown).

To measure downstream MAP kinase activity, human granulocytes from normal volunteers were resuspended in RPMI-1640 (Invitrogen) at 10×10^6 mL^{-1} and were stimulated with 1 μg/mL hS100A7 ± 15nM $ZnCl_2$ at 37°C for 5 min before being pelleted followed by removal of media. The pellets were quick frozen in a dry ice/methanol bath. Cells were preincubated with neutralizing anti-RAGE (5 μg/mL, R&D, Minneapolis, MN) or soluble RAGE (R&D) 30 min prior to stimulation.

For immunoblot analysis, total cell lysates of neutrophils, CHO cells or cultured keratinocytes (20 μg) were prepared using 1% Triton-containing lysis buffer (Cell Signaling). Proteins were separated using a 12% SDS-polyacrylamide gel, transferred to reinforced nitrocellulose membranes and visualized by Ponceau stain. Filters were incubated with blocking buffer (TBS, pH 7.4, with 5% milk, 0.1% Tween 20) for 30 min, primary antibody (anti-hS100A15, 1μg/mL; anti-hS100A7 antibody, 1μg/mL; anti-phospho-ERK1/2, anti-total ERK1/2, 1:1000, Cell Signaling; anti-RAGE, 1:250, Santa Cruz, Santa Cruz, CA; anti-β actin, 1:20,000 Chemicon, Temecula, CA) overnight, and secondary antibody for 1 h with several washes (TBS, pH 7.4, 0.1% Tween 20) between incubations.

Immunoflorescent staining was performed on serial 5 μm frozen sections of human normal and psoriatic skin fixed in acetone. The sections were treated with 96% methanol and 4% hydrogen peroxide, blocked in 10% normal goat serum, and incubated overnight with anti-hS100A15 or anti-hS100A7 (5 μg/ml each). Experiments without primary antibodies and serial dilution competition assays were performed in the absence and presence of blocking peptide to determine the optimal working concentration and specificity of the primary hS100A15 antibody. Donkey anti-rabbit cy3 (1:250) was used as a secondary antibody to the hS100A15 or donkey anti-mouse FITC (1:250) to hS100A7 (Jackson Laboratory, Bar Harbor, MI). When sections were co-stained, FITC-labeled Mart-1/Hmb 45 cocktail at1:25 dilution (Monoclonal Biocare Medical, Concord, CA) and MHCII-FITC at 1:250 dilution (Serotec, Raleigh, NC) were mixed with the primary antibody. All sections were nuclear stained with DAPI (Sigma) and mounted. All biopsies were taken with the patient's informed consent and approval of the local ethics committee.

Chemotaxis assays

Human leukocytes from normal volunteers were percoll-purified (95%) from leukopacs provided by the NIH blood bank (under IRB 99-CC-0168) as previously described 14. The chemoattractants hS100A7, hS100A15, and CXCL8/IL-8 (PeproTech, Rocky Hill, NJ) were diluted in RPMI 1640 containing 1% bovine serum albumin and placed in the lower 25 μL chamber. hS100A7 was mixed with $ZnCl_2$ at least 30 min prior being placed in a chemotaxis chamber. Cells were suspended in the above medium at $0.5–5 \times 10^6$ mL^{-1} and 50 μL were placed in the upper chamber, which was separated from the lower one by a polycarbonate filter (pore size: 5 μm), which was coated with fibronectin for lymphocyte migration. In selected experiments, neutralizing anti-hRAGE (5 μg/mL), pertussis toxin (50–100 ng/mL), CXCL12 (PeproTech, Rocky Hill, NJ), PD98059 (10 μM), hS100A7 or hS100A15 was added 30 min at 37C prior to the cells being added in the upper chamber. Cells were allowed to migrate for 3h (T-lymphocytes), 1h (granulocytes), or 1.5h (monocytes) at 37°C in a humidified, 5% CO_2 incubator. Cells attached to the lower filter surface were stained Rapid Stain (Richard Allen, Kalamazoo, MI), counted in six fields and the averages were expressed as ratio

(chemotactic index) of the numbers of cells in the treated sample versus control (spontaneous migration).

In vitro ligand-receptor interactions

Recombinant hS100A7 was biotinylated using N-hydroxysuccinimide ester of biotin (NHS-PEO_4-Biotin) containing polyethylene glycol spacer arm that renders/maintains hS100A7 aqueous solubility. hS100A7 (2 mg) dissolved in PBS (0.1 M Phosphate, 0.15 M NaCl, pH 7.2) was mixed with 2 molar excess of NHS-PeO_4-biotin and incubated on ice for 2 hr. Biotinylated-S100A7 (Biotin-S100A7) was separated from unreacted NHS-PEO_4-biotin using Econo-Pac 10 DG column (Bio-Rad, Hercules, CA) and stored at –80°C until use. Ligand binding assays were performed in 96-well polystyrene plates which were preadsorbed with purified murine recombinant soluble RAGE (100 ng/well) overnight and blocked with 0.25% casein (I-block) (AppIied Biosystems, Foster City, CA). Assays were performed in the presence of the indicated concentration of biotinylated hS100A7 ± excess of unlabeled recombinant hS100A7, hS100A15, non-immune IgG (Jackon Laboratories), anti-mouse RAGE (R&D), anti-human RAGE (R&D), sRAGE (R&D), CXCL8/IL-8 or I-block in PBS (1 mM KH_2PO_4, 3 mM Na_2HPO_4, 155 mM NaCl, 1.2 mM $CaCl_2$, 50 μM $ZnCl_2$) for 90 min at 37°C. Wells were washed rapidly to remove unbound ligand, then incubated with streptavidin alkaline phosphatase (1:1500 dilution) in I-block at room temperature for 60 min, and washed with PBST, distilled water, and Tris buffer (20 mM Tris, 1 mM $MgCl_2$, pH 9.5) before adding CDP-Star containing Emerald II enhancer and incubating at room temperature for 20 min and at 4°C overnight. Luminescence was measured using a TR717 Microplate Luminometer (PE Applied Biosystems, Foster City, CA). Binding of biotin-S100A7 to RAGE is directly proportional to the amount of luminescence signal in the well and is reported as luminescence units (LU). High binding polystyrene 96-well plates were obtained from Greiner Bio-one (Longwood, FL), streptavidine-alkaline phosphatase, I block (casein) and chemiluminescent substrate (CDP-Star containing Emerald II enhancer) were obtained from PE Applied Biosystems (Foster City, CA), and NHS-PEO_4-Biotin was from Pierce (Rockford, IL).

Cell adhesion assays

Control vector or RAGE transfected Chinese hamster ovary (CHO) cells were allowed to adhere to immobilized hS100A7, hS100A15 (10 μg/mL each) and to bovine serum albumin (as control) according to a previously described modified protocol 15. Briefly, microtiter plates were coated with the S100 proteins in bicarbonate buffer, pH 9.6, and blocked with 3% BSA solution. Fluorescently labeled (BCECF AM) CHO control or RAGE-vector transfected cells were washed in serum-free RPMI medium and plated onto the precoated wells (10^5/well) at 37°C for 60 min in the absence or presence of zinc (50 μM) or neutralizing anti-RAGE or sRAGE (5 μg/mL, R&D). After the 60 min incubation period, the wells were washed and adherent cells were quantified by measuring absorbance at 590 nm.

In vivo peritonitis model

C57/BL6 RAGE−/− mice were characterized previously15. HBSS (Invitrogen), recombinant native or heat-inactivated S100 proteins (20 μg in 1 mL HBSS/mouse) [16;17] were administered intraperitoneally into C57/BL6 wild-type and RAGE −/− mice. As control, thioglycollate-induced peritonitis was performed as previously described 12. To evaluate neutrophil recruitment, mice were sacrificed at 4 h after injection. Thereafter, the peritoneal lavage was collected and the number of emigrated cells was analyzed by hemocytometry. There was no difference in the circulating neutrophil count of wild-type or RAGE−/− mice. Recovered peritoneal leukocytes were incubated for 5 min with 2.3G2 anti-FcIII/II receptor, then stained at 4°C for 30 min with allophycocyanin-conjugated anti-Gr1 as a neutrophil marker. Cells were fixed with 1% paraformaldehyde, and cytometry was done with a FACS Caliber Cytometer

(Becton-Dickinson Biosciences, Franklin Lakes, NJ) and results were analyzed with Diva-Software (Becton-Dickinson Biosciences). Similar results were obtained by analyzing leukocyte populations with conventional smears. All antibodies were purchased from BD Pharmingen.

Bioinformatics

The amino acid sequences of the human S100 proteins were aligned using the program T-Coffee (version 2.11).

Statistical analysis

Data were analyzed for statistical significance by ANOVA with post-hoc Bonferroni analysis using SPSS (version 15.0) with $P \leq 0.05$ being considered significant.

Results

hS100A7 and hS100A15 paralogs are differentially expressed

Because hS100A7 and hS100A15 are almost identical in sequence (93%), distinguishing their expression has been difficult (Fig. 1A). To address this further, antibodies were generated in rabbits to a unique N-terminal sequence in human S100A15 (hS100A15). Immunoblotting revealed a single monomer band of recombinant hS100A15 distinct from other S100 proteins and native low- and high-molecular weight bands in keratinocyte lysates as is typical for many S100 proteins 4 (Fig. 1A). The hS100A15 antibody did not detect related recombinant hS100 proteins, particularly hS100A7. Similarly, the monoclonal hS100A7 antibody revealed specific staining of the hS100A7 monomer along with high molecular weigh forms in keratinocyte lysates that were distinct from those detected with the hS100A15 antibody.

Using these specific antibodies, the expression and distribution of the corresponding hS100A7 and hS100A15 proteins in human skin was studied. In normal epidermis, hS100A7 expression was confined to the granular/cornified layer only (Fig. 1B, upper left panel). Human S100A15 co-localized there but unlike hS100A7, it was expressed by epidermal basal cells and dendritic-shaped cells (Fig. 1B, upper right panel). By co-staining, these hS100A15 expressing dendritic cells were identified as melanocytes (MART-1 positive), whereas MART-1 negative, hS100A15 positive cells were identified as epidermal Langerhans cells (Fig. 1B, lower left panel) and dermal dendritic cells (MHCII positive, not shown). In the dermis, hS100A15 was further expressed by endothelial cells interior to vascular smooth muscle cells (smooth muscle actin positive) (Fig. 1B, lower right panel) and other cell types, where hS100A7 and hS100A15 were differentially expressed (summarized in Fig. 1C).

Since psoriasis is the prototype of inflammatory disease where hS100A7 and hS100A15 were first identified, our unique hS100A15 antibody provided an opportunity to discriminate the expression of these proteins in psoriatic skin (Fig. 1D). Compared with normal skin, both hS100A7 and hS100A15 are upregulated in inflamed lesional psoriatic skin and co-expressed by the epidermal suprabasal compartments. In addition, hS100A15 is highly expressed by basal psoriatic keratinocytes at the epidermal-stroma junction, as well as dendritic and stromal cells in the dermis. Their differential expression in multiple cell types in different compartments of the skin might reflect their divergence and functional synergism with implications for disease pathogenesis.

Both hS100A7 and hS100A15 are chemoattractants *in vitro*, but differ in cell targets and receptor activation

Both human S100A7 and S100A15 were identified in psoriasis and upregulated in psoriasis, suggesting involvement in the inflammatory phenotype[1;6]. To investigate the possibility that

these proteins attracted some of the inflammatory cells, we analyzed the chemotactic ability of hS100A7 and hS100A15 in a dual chamber assay (Fig. 2A). hS100A15 was identified as chemotactic for both granulocytes and monocytes, but not lymphocytes. In contrast, hS100A7 attracted all three leukocyte populations at similar concentrations. In both cases, chemotaxis diminished at 100 ng/mL developing an overall bell-shaped response that is typical for chemokines 18. To examine the role for a Gi protein-coupled receptor (GiPCR) in the chemotactic response, the assay was performed in the presence of pertussis toxin (Fig. 2B). hS100A15 mediated chemotaxis was attenuated upon pertussis-toxin treatment indicating signaling through a GiPCR. In contrast, pertussis toxin did not affect the hS100A7-induced neutrophil migration. As a positive control for the assay, IL-8 chemotaxis, mediated by the Gi-protein coupled receptor CXCR1/2, was reduced by the pertussis-toxin treatment.

A series of additional studies were performed to further elucidate the nature of the chemotactic receptors (Fig. 2C). hS100A7-mediated chemotaxis could be inhibited by the specific anti-hS100A7 antibody but could not be desensitized through activation of the classical pertussis toxin sensitive interaction of CXCL12 with CXCR4. In contrast, blocking of the Receptor of Advanced Glycated End Products (RAGE) by neutralizing antibodies abolished the hS100A7-mediated chemotaxis, but not the IL-8 mediated effect. To confirm a role of RAGE receptor in hS100A7-mediated chemotaxis, hS100A7 was placed in the bottom chamber and normal RAGE-bearing granulocytes were added to the upper chamber (Fig. 2D). When neutralizing anti-RAGE was added to the cells, hS100A7-mediated cell migration was inhibited, excluding undirected chemokinesis. In contrast, cell migration towards hS100A15 placed in the lower chamber was not affected by blocking RAGE on granulocytes in the upper chamber. Further, checkerboard analysis showed that hS100A7 and hS100A15 pro-migratory effects are mediated through chemotaxis (data not shown). To address the nature of the pertussis toxin sensitive hS100A15 receptor, desensitization experiments with ligands were performed that signal through GiPCR. Pretreatment of neutrophils with the ligands RANTES/CCL5, SDF-1/CXCL12, MCP-1/CCL2 and IL-8/CXCL8 did not attenuate the hS100A15-mediated chemotaxis as opposed to corresponding ligand controls (data not shown). Due to the myeloid preference of hS100A15 and inability to attract mature or immature dendritic cells and lymphocytes, chemokine receptors that are preferentially expressed on lymphocytes or dendritic cells were excluded as potential targets for hS100A15 (CXCR 3, 5, 6; CCR 4, 6–10). BRAK/CXCL14 ligand [18;19], which binds to an as yet unknown chemokine receptor(s) was able to desensitize hS100A15 mediated monocyte chemotaxis, whereas hS100A15 did not desensitize the chemotactic response to CXCL14 (data not shown). This unidirectional desensitization is probably based on the greater potency of CXCL14 than hS100A15.

To directly test the concept of hS100A7 and hS100A15 binding to different target receptors, ligand binding studies were performed (Fig. 3A). Biotinylated hS100A7 bound to immobilized purified RAGE, and binding could be blocked by increasing concentrations of unlabeled hS100A7. Biotinylated hS100A7 binding to RAGE substrate was inhibited in the presence of excess soluble RAGE (sRAGE), a truncated form of the receptor spanning the extracellular domain, and by anti-human and anti-mouse RAGE-IgG as well as anti-hS100A7. Unrelated casein or non-immune IgG was without effect as was competition with increasing concentrations of the hS100A15 paralog or IL-8.

Structural and biochemical data indicate that the S100A7 homodimer structure is altered through the binding and release of zinc, an important mediator in inflammation [20;21]. To test if zinc affects the hS100A7-RAGE interaction and function, hS100A7-mediated ligand binding, signaling and chemotaxis were analyzed. Ligand binding experiments with RAGE in a natural cellular environment showed that adhesion of RAGE-transfected CHO cells to hS100A7-coated wells required zinc (Fig. 3B). The specificity of RAGE-hS100A7 interaction was shown by inhibition in the presence of excess soluble RAGE (sRAGE) or neutralizing

anti-RAGE IgG. Further, the presence of zinc did not affect the lack of binding of RAGE-bearing cells towards plates coated with hS100A15. RAGE-deficient CHO cells transfected with a vector control did not adhere to plates coated with either S100 protein. Human neutrophils exposed to a gradient of recombinant hS100A7 protein in the absence of zinc, showed no significant chemotactic response. The ability of hS100A7 to attract neutrophils was restored upon zinc replenishment (Fig. 3C). In line with zinc-dependent hS100A7-RAGE interaction and chemotaxis, neutrophils stimulated with hS100A7 showed RAGE-dependent phosphorylation of the migration-related MAPK ERK1/2 pathway 22 only in the presence of zinc (Fig. 3D). hS100A7-induced ERK1/2 phosphorylation was blocked by sRAGE (not shown) or neutralizing anti-RAGE IgG. The hS100A7-mediated chemotaxis was attenuated when neutrophils were pretreated with an ERK1/2 inhibitor, similar to IL-8 (Fig. 3E), indicating the requirement for ERK1/2 signaling for chemotactic response to hS100A7.

hS100A7 and hS100A15 are proinflammatory and synergistic *in vivo* but differ in receptor specificity

To test the concept that both hS100A7 and hS100A15 are chemoattractants *in vivo*, corresponding recombinant proteins were injected intraperitoneally into C57/BL6 mice. Proinflammatory response was evaluated by analyzing cell count and cell type attracted into the peritoneal cavity. Both S100 proteins provoked an inflammatory response that was dose- and time-dependent and was absent when heat-inactivated S100 proteins were injected (not shown). In C57/BL6 wild type mice, a response was detected by four hours for both proteins attracting Gr-1 positive cells compared with control (Fig. 4A). The hS100A7-induced inflammation was absent in RAGE −/− mice, whereas the hS100A15-mediated inflammatory response remained intact. As a positive control, intraperitoneally injected MIP-2/mCXCL2 provoked an inflammation in both wild type and RAGE −/− mice.

Since we found that hS100A7 and hS100A15 have distinct proinflammatory functions mediated through distinct mechanisms but are expressed in different compartments in the same inflammatory states, we tested for their combined effect as chemoattractants (Fig. 4B). Although intraperitoneal application of either hS100A7 or hS100A15 provoked an inflammatory response (compare Fig. 4A), this was amplified substantially when both hS100A7 and hs100A15 were injected together. Thus, hS100A7 and hS100A15 act synergistically when co-expressed (Fig. 1D), suggesting that both proteins might contribute to the amplified inflammatory phenotype in psoriasis and other inflammatory diseases.

Discussion

Originally identified as a marker for psoriasis, hS100A7 (psoriasin)1 and recently hS100A156 were found overexpressed in other inflammatory diseases23–25. Physiologically, hS100A7 and hS100A15 may work together as part of an innate host defense controlling microbial growth on normal and inflamed skin [13;26–28]. Our current data indicate another function as chemoattractants for leukocytes. hS100A7 13 and hS100A15 25 are both regulated by proinflammatory cytokines that are predominant in inflammatory diseases, such as psoriasis [29;30]. That they are co-evolved, co-expressed and co-regulated in identical pathological states begs the question of the biological significance of the evolutionary selection for these almost identical proteins.

Our data suggest a joint biological impact of hS100A7 and hS100A15 through evolutionary diversification. Both proteins are distinct in expression pattern, chemotactic activity and functional mechanism. While each of them induces a proinflammatory response by itself, their proinflammatory activity is potentiated when acting together indicating that they contribute independently but synergistically to inflammation that may be fundamental to the disease phenotype. We provide mechanistic insights into hS100A7 and hS100A15 synergism by

showing their biological diversity in expression in distinct cells in both normal and inflamed tissue, in receptor activation and in chemotactic function. The documented upregulation of hS100A7 in epithelial cancers 31 and similar findings for hS100A15 (unpublished) suggest that combined expression of these chemotactic proteins may contribute to other diseases as well. Having established specific antibodies for each protein, we are now in a position to address this question. Further, parallel targeting of hS100A7 and hS100A15 would allow a novel approach to treat associated diseases based on distinct mechanisms with possibly enhanced therapeutic efficacy [32;33].

With the discovery of hS100A7 in 1991, structural and functional data have stimulated the quest for mechanistic clarification of its extracellular action [21;34]. The multiligand receptor RAGE is implicated in inflammatory processes including leukocyte migration[12;15;35;36]. RAGE is expressed at low levels in normal tissues and becomes upregulated wherever its ligands accumulate. Ligands initiate a sustained cellular activation through MAP-kinases culminating in the activation of NFκB [37;38]. Through recognition of β-sheet fibrillar structures or proinflammatory cytokine-like mediators of the S100/calgranulin family or high mobility group box-1 (HMGB-1), RAGE participates in the phenotype of inflammatory skin diseases, diabetes, amyloidosis and promotes tumor progression [37;39–43]. The identification of RAGE as a receptor for hS100A7 allows for specific targeting of hS100A7 mediated effects, such as cell migration in inflammation. Further, with participation of RAGE in tumor growth and metastasis43, hS100A7-RAGE interaction might be important to understand the role of secreted hS100A7 in epithelial tumorigenesis.

In contrast to hS100A7, hS100A15 preferentially attracts myeloid cells through a pertussis toxin-sensitive mechanism suggesting signaling through a GiPCR. Two other chemotactic S100 proteins, S100-L and CP-10, bind to pertussis toxin-sensitive receptors, which, however, are yet to be identified [44;45]. Similar to CP-10, calcium mobilization through hS100A15 could not be detected (not shown). This observation is consistent with the idea that S100 proteins are less potent than the classical chemoattractants. Homologous desensitization experiments with chemokine receptor ligands suggest that receptors preferentially active on myeloid cells (CXCR1/2, CCR1) or widespread receptors (CXCR4; CCR2, 3, 5) are not involved in hS100A15-mediated chemotaxis. Together, our data suggest that hS100A15 binds to an unidentified GiPCR which also interacts with CXCL14.

hS100A15 is functionally active in the presence of calcium alone compared to hS100A7, suggesting additional factors are important for hS100A7 chemotactic activity. Besides calcium, many S100 proteins bind zinc with high affinity, implying that divalent zinc is a major regulator of their extracellular function [13;20;21;46]. In hS100A7 21 and others [37;46;47], the location of the zinc binding site is near one of the proposed target protein binding sites, however mechanistic and functional consequences are undefined. We demonstrate that zinc is required for interaction and signaling of hS100A7 with the target protein RAGE, and is functionally important for hS100A7-RAGE mediated chemotaxis. Thus, our data indicate that zinc is a necessary co-factor for hS100A7-mediated proinflammatory activity. Together with previous studies [13;26–28] showing that the antimicrobial action of hS100A7 was through zinc sequestration, we suggest that zinc may be involved in regulation of hS100A7 dual proinflammatory and antimicrobial functions.

For S100 proteins, individual physical and biochemical characteristics including the spatial structure of the S100 dimer/multimers determine the specificity of the target interaction [7;48;49]. We have data suggesting that sequences and secondary structures of the hS100A7 and hS100A15 monomers are alike[6;11]. However, the quaternary structures of both proteins are distinct and could account for binding to different target receptors (Ahvazi et al., unpublished data). Further, two of the amino acids divergent in hS100A7 and hS100A15 (Thr52Ileu,

Asn53His) appear to reside in a region that was shown to be a chemotactic domain for mouse S100A8 50. If functionally conserved in hS100A7 and hS100A15, these differences might contribute as well to the distinct chemotactic properties of these highly homologous proteins.

Understanding the diversity and functional synergism of disease-associated proteins is crucial for developing therapeutic interventions based on distinct mechanisms with possibly enhanced therapeutic efficiency in S100A7- and S100A15- mediated pathological conditions. The unexpected different biology of almost identical proteins suggests that S100A7 and hS100A15 functional synergisms through biological diversification might underlie their biological impact, and thus their evolutionary selection.

Acknowledgements

Grant support: Ronald Wolf is funded by the German Research Foundation (DFG), Emmy-Noether Program (Wo 843/2-1). This research was supported in part by the Intramural Research Program of the National Cancer Institute, Center for Cancer Research, and of the National Institute of Arthritis and Musculoskeletal and Skin Diseases of the National Institutes of Health.

We are grateful to Stephen Wincovitch and Susan Garfield for skillful assistance with confocal microscopy and Barbara Taylor for advice and help with the flow cytometry. We thank William Gillette and Jim Hartley for recombinant proteins, Roberta Smith for quantitative cell analysis and Helen Rager for endotoxin analysis. We thank Christophe Cataisson for skillful help with the in vivo experiments and critical reading of the manuscript. We thank Alif Dharamsi for competent technical assistance, Peter Nawroth and Angelika Bierhaus for providing RAGE−/− mice.

abbreviations

BCECF AM
: 2′,7′-bis-(2-carboxyethyl)-5-(and-6)-carboxyfluorescein, acetoxymethyl ester

GiPCR
: Gi protein-coupled receptor

Reference List

1. Madsen P, Rasmussen HH, Leffers H, Honore B, Dejgaard K, Olsen E, Kiil J, Walbum E, Andersen AH, Basse B. Molecular cloning, occurrence, and expression of a novel partially secreted protein “psoriasin” that is highly up-regulated in psoriatic skin. J Invest Dermatol 1991;97:701–712. [PubMed: 1940442]
2. Boniface K, Bernard FX, Garcia M, Gurney AL, Lecron JC, Morel F. IL-22 inhibits epidermal differentiation and induces proinflammatory gene expression and migration of human keratinocytes. J Immunol 2005;174:3695–3702. [PubMed: 15749908]
3. Boniface K, Diveu C, Morel F, Pedretti N, Froger J, Ravon E, Garcia M, Venereau E, Preisser L, Guignouard E, Guillet G, Dagregorio G, Pene J, Moles JP, Yssel H, Chevalier S, Bernard FX, Gascan H, Lecron JC. Oncostatin M secreted by skin infiltrating T lymphocytes is a potent keratinocyte activator involved in skin inflammation. J Immunol 2007;178:4615–4622. [PubMed: 17372020]
4. Eckert RL, Broome AM, Ruse M, Robinson N, Ryan D, Lee K. S100 proteins in the epidermis. J Invest Dermatol 2004;123:23–33. [PubMed: 15191538]
5. Wolk K, Witte E, Wallace E, Docke WD, Kunz S, Asadullah K, Volk HD, Sterry W, Sabat R. IL-22 regulates the expression of genes responsible for antimicrobial defense, cellular differentiation, and mobility in keratinocytes: a potential role in psoriasis. Eur J Immunol 2006;36:1309–1323. [PubMed: 16619290]
6. Wolf R, Mirmohammadsadegh A, Walz M, Lysa B, Tartler U, Remus R, Hengge U, Michel G, Ruzicka T. Molecular cloning and characterization of alternatively spliced mRNA isoforms from psoriatic skin encoding a novel member of the S100 family. FASEB J 2003;17:1969–1971. [PubMed: 12923069]
7. Donato R. Intracellular and extracellular roles of S100 proteins. Microsc Res Tech 2003;60:540–551. [PubMed: 12645002]

8. Heizmann CW, Fritz G, Schafer BW. S100 proteins: structure, functions and pathology. Front Biosci 2002;7:d1356–d1368. [PubMed: 11991838]
9. Kulski JK, Lim CP, Dunn DS, Bellgard M. Genomic and phylogenetic analysis of the S100A7 (Psoriasin) gene duplications within the region of the S100 gene cluster on human chromosome 1q21. J Mol Evol 2003;56:397–406. [PubMed: 12664160]
10. Wolf R, Voscopoulos CJ, FitzGerald PC, Goldsmith P, Cataisson C, Gunsior M, Walz M, Ruzicka T, Yuspa SH. The mouse S100A15 ortholog parallels genomic organization, structure, gene expression, and protein-processing pattern of the human S100A7/A15 subfamily during epidermal maturation. J Invest Dermatol 2006;126:1600–1608. [PubMed: 16528363]
11. Boeshans KM, Wolf R, Voscopoulos C, Gillette W, Esposito D, Mueser TC, Yuspa SH, Ahvazi B. Purification, crystallization and preliminary X-ray diffraction of human S100A15. Acta Crystallograph Sect F Struct Biol Cryst Commun 2006;62:467–470.
12. Orlova VV, Choi EY, Xie C, Chavakis E, Bierhaus A, Ihanus E, Ballantyne CM, Gahmberg CG, Bianchi ME, Nawroth PP, Chavakis T. A novel pathway of HMGB1-mediated inflammatory cell recruitment that requires Mac-1-integrin. EMBO J 2007;26:1129–1139. [PubMed: 17268551]
13. Glaser R, Harder J, Lange H, Bartels J, Christophers E, Schroder JM. Antimicrobial psoriasin (S100A7) protects human skin from Escherichia coli infection. Nat Immunol 2005;6:57–64. [PubMed: 15568027]
14. Chertov O, Ueda H, Xu LL, Tani K, Murphy WJ, Wang JM, Howard OM, Sayers TJ, Oppenheim JJ. Identification of human neutrophil-derived cathepsin G and azurocidin/CAP37 as chemoattractants for mononuclear cells and neutrophils. J Exp Med 1997;186:739–747. [PubMed: 9271589]
15. Chavakis T, Bierhaus A, Al Fakhri N, Schneider D, Witte S, Linn T, Nagashima M, Morser J, Arnold B, Preissner KT, Nawroth PP. The pattern recognition receptor (RAGE) is a counterreceptor for leukocyte integrins: a novel pathway for inflammatory cell recruitment. J Exp Med 2003;198:1507–1515. [PubMed: 14623906]
16. Foell D, Wittkowski H, Vogl T, Roth J. S100 proteins expressed in phagocytes: a novel group of damage-associated molecular pattern molecules. J Leukoc Biol 2007;81:28–37. [PubMed: 16943388]
17. Harrison CA, Raftery MJ, Walsh J, Alewood P, Iismaa SE, Thliveris S, Geczy CL. Oxidation regulates the inflammatory properties of the murine S100 protein S100A8. J Biol Chem 1999;274:8561–8569. [PubMed: 10085090]
18. Oppenheim JJ, Yang D, Biragyn A, Howard OM, Plotz P. Chemokine receptors on dendritic cells promote autoimmune reactions. Arthritis Res 2002;4(Suppl 3):S183–S188. [PubMed: 12110138]
19. Hromas R, Broxmeyer HE, Kim C, Nakshatri H, Christopherson K, Azam M, Hou YH. Cloning of BRAK, a novel divergent CXC chemokine preferentially expressed in normal versus malignant cells. Biochem Biophys Res Commun 1999;255:703–706. [PubMed: 10049774]
20. Vorum H, Madsen P, Rasmussen HH, Etzerodt M, Svendsen I, Celis JE, Honore B. Expression and divalent cation binding properties of the novel chemotactic inflammatory protein psoriasin. Electrophoresis 1996;17:1787–1796. [PubMed: 8982613]
21. Brodersen DE, Nyborg J, Kjeldgaard M. Zinc-binding site of an S100 protein revealed. Two crystal structures of Ca2+-bound human psoriasin (S100A7) in the Zn2+-loaded and Zn2+-free states. Biochemistry 1999;38:1695–1704. [PubMed: 10026247]
22. Nakamae-Akahori M, Kato T, Masuda S, Sakamoto E, Kutsuna H, Hato F, Nishizawa Y, Hino M, Kitagawa S. Enhanced neutrophil motility by granulocyte colony-stimulating factor: the role of extracellular signal-regulated kinase and phosphatidylinositol 3-kinase. Immunology 2006;119:393–403. [PubMed: 16903868]
23. Algermissen B, Sitzmann J, LeMotte P, Czarnetzki B. Differential expression of CRABP II, psoriasin and cytokeratin 1 mRNA in human skin diseases. Arch Dermatol Res 1996;288:426–430. [PubMed: 8844119]
24. Di Nuzzo S, Sylva-Steenland RM, Koomen CW, de Rie MA, Das PK, Bos JD, Teunissen MB. Exposure to UVB induces accumulation of LFA-1+ T cells and enhanced expression of the chemokine psoriasin in normal human skin. Photochem Photobiol 2000;72:374–382. [PubMed: 10989609]

25. Wolf R, Lewerenz V, Buchau AS, Walz M, Ruzicka T. Human S100A15 splice variants are differentially expressed in inflammatory skin diseases and regulated through Th1 cytokines and calcium. Exp Dermatol 2007;16:685–691. [PubMed: 17620096]
26. Buchau AS, Hassan M, Kukova G, Lewerenz V, Kellermann S, Wurthner JU, Wolf R, Walz M, Gallo RL, Ruzicka T. S100A15, an Antimicrobial Protein of the Skin: Regulation by E. coli through Toll-Like Receptor 4. J Invest Dermatol. 2007
27. Lee KC, Eckert RL. S100A7 (Psoriasin)--mechanism of antibacterial action in wounds. J Invest Dermatol 2007;127:945–957. [PubMed: 17159909]
28. Schroder JM, Harder J. Antimicrobial skin peptides and proteins. Cell Mol Life Sci 2006;63:469–486. [PubMed: 16416029]
29. Griffiths CE. The immunological basis of psoriasis. J Eur Acad Dermatol Venereol 2003;17(Suppl 2):1–5. [PubMed: 12795768]
30. Lew W, Bowcock AM, Krueger JG. Psoriasis vulgaris: cutaneous lymphoid tissue supports T-cell activation and “Type 1” inflammatory gene expression. Trends Immunol 2004;25:295–305. [PubMed: 15145319]
31. Al Haddad S, Zhang Z, Leygue E, Snell L, Huang A, Niu Y, Hiller-Hitchcock T, Hole K, Murphy LC, Watson PH. Psoriasin (S100A7) expression and invasive breast cancer. Am J Pathol 1999;155:2057–2066. [PubMed: 10595935]
32. Daly C, Rollins BJ. Monocyte chemoattractant protein-1 (CCL2) in inflammatory disease and adaptive immunity: therapeutic opportunities and controversies. Microcirculation 2003;10:247–257. [PubMed: 12851642]
33. Luster AD, Alon R, von Andrian UH. Immune cell migration in inflammation: present and future therapeutic targets. Nat Immunol 2005;6:1182–1190. [PubMed: 16369557]
34. Jinquan T, Vorum H, Larsen CG, Madsen P, Rasmussen HH, Gesser B, Etzerodt M, Honore B, Celis JE, Thestrup-Pedersen K. Psoriasin: a novel chemotactic protein. J Invest Dermatol 1996;107:5–10. [PubMed: 8752830]
35. Bierhaus A, Humpert PM, Morcos M, Wendt T, Chavakis T, Arnold B, Stern DM, Nawroth PP. Understanding RAGE, the receptor for advanced glycation end products. J Mol Med 2005;83:876–886. [PubMed: 16133426]
36. Schmidt AM, Yan SD, Yan SF, Stern DM. The multiligand receptor RAGE as a progression factor amplifying immune and inflammatory responses. J Clin Invest 2001;108:949–955. [PubMed: 11581294]
37. Hofmann MA, Drury S, Fu C, Qu W, Taguchi A, Lu Y, Avila C, Kambham N, Bierhaus A, Nawroth P, Neurath MF, Slattery T, Beach D, McClary J, Nagashima M, Morser J, Stern D, Schmidt AM. RAGE mediates a novel proinflammatory axis: a central cell surface receptor for S100/calgranulin polypeptides. Cell 1999;97:889–901. [PubMed: 10399917]
38. Sorci G, Riuzzi F, Agneletti AL, Marchetti C, Donato R. S100B inhibits myogenic differentiation and myotube formation in a RAGE-independent manner. Mol Cell Biol 2003;23:4870–4881. [PubMed: 12832473]
39. Deane R, Du YS, Submamaryan RK, LaRue B, Jovanovic S, Hogg E, Welch D, Manness L, Lin C, Yu J, Zhu H, Ghiso J, Frangione B, Stern A, Schmidt AM, Armstrong DL, Arnold B, Liliensiek B, Nawroth P, Hofman F, Kindy M, Stern D, Zlokovic B. RAGE mediates amyloid-beta peptide transport across the blood-brain barrier and accumulation in brain. Nat Med 2003;9:907–913. [PubMed: 12808450]
40. Dumitriu IE, Baruah P, Manfredi AA, Bianchi ME, Rovere-Querini P. HMGB1: guiding immunity from within. Trends Immunol 2005;26:381–387. [PubMed: 15978523]
41. Lotze MT, Tracey KJ. High-mobility group box 1 protein (HMGB1): nuclear weapon in the immune arsenal. Nat Rev Immunol 2005;5:331–342. [PubMed: 15803152]
42. Park L, Raman KG, Lee KJ, Lu Y, Ferran LJ Jr, Chow WS, Stern D, Schmidt AM. Suppression of accelerated diabetic atherosclerosis by the soluble receptor for advanced glycation endproducts. Nat Med 1998;4:1025–1031. [PubMed: 9734395]
43. Taguchi A, Blood DC, del Toro G, Canet A, Lee DC, Qu W, Tanji N, Lu Y, Lalla E, Fu C, Hofmann MA, Kislinger T, Ingram M, Lu A, Tanaka H, Hori O, Ogawa S, Stern DM, Schmidt AM. Blockade

of RAGE-amphoterin signalling suppresses tumour growth and metastases. Nature 2000;405:354–360. [PubMed: 10830965]

44. Cornish CJ, Devery JM, Poronnik P, Lackmann M, Cook DI, Geczy CL. S100 protein CP-10 stimulates myeloid cell chemotaxis without activation. J Cell Physiol 1996;166:427–437. [PubMed: 8592003]
45. Komada T, Araki R, Nakatani K, Yada I, Naka M, Tanaka T. Novel specific chemtactic receptor for S100L protein on guinea pig eosinophils. Biochem Biophys Res Commun 1996;220:871–874. [PubMed: 8607858]
46. Miranda LP, Tao T, Jones A, Chernushevich I, Standing KG, Geczy CL, Alewood PF. Total chemical synthesis and chemotactic activity of human S100A12 (EN-RAGE). FEBS Lett 2001;488:85–90. [PubMed: 11163801]
47. Xie J, Burz DS, He W, Bronstein IB, Lednev I, Shekhtman A. Hexameric Calgranulin C (S100A12) Binds to the Receptor for Advanced Glycated End Products (RAGE) Using Symmetric Hydrophobic Target-binding Patches. J Biol Chem 2007;282:4218–4231. [PubMed: 17158877]
48. Santamaria-Kisiel L, Rintala-Dempsey AC, Shaw GS. Calcium-dependent and -independent interactions of the S100 protein family. Biochem J 2006;396:201–214. [PubMed: 16683912]
49. Zimmer DB, Wright SP, Weber DJ. Molecular mechanisms of S100-target protein interactions. Microsc Res Tech 2003;60:552–559. [PubMed: 12645003]
50. Ravasi T, Hsu K, Goyette J, Schroder K, Yang Z, Rahimi F, Miranda LP, Alewood PF, Hume DA, Geczy C. Probing the S100 protein family through genomic and functional analysis. Genomics 2004;84:10–22. [PubMed: 15203200]

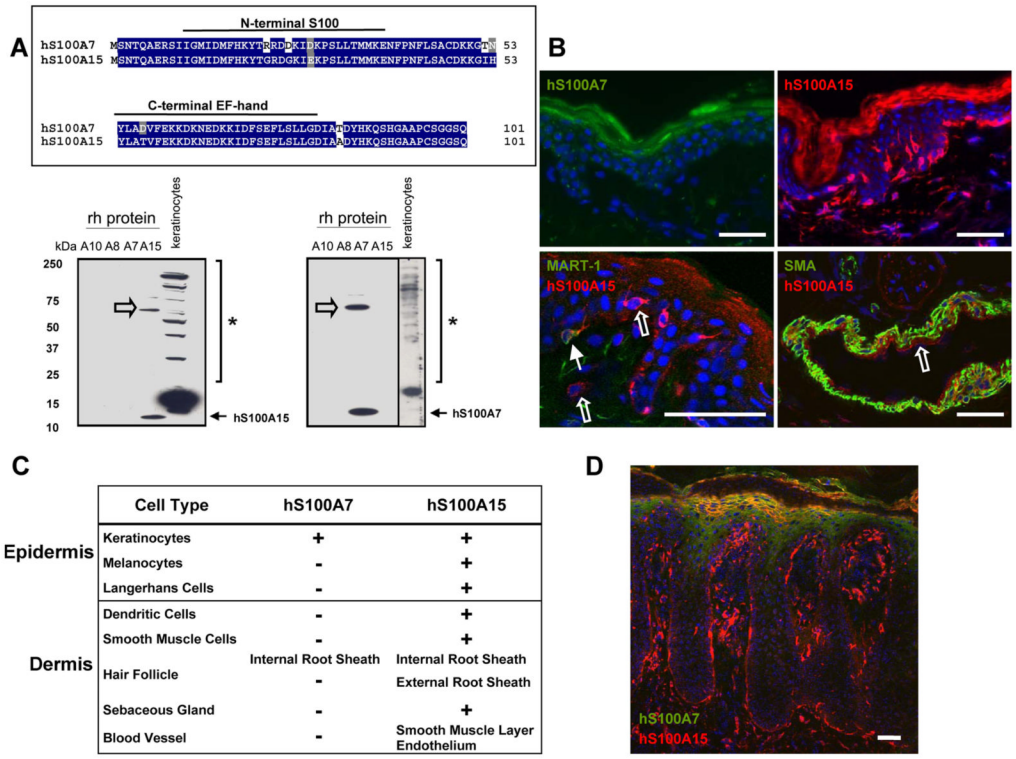

FIGURE 1. Human S100A7 and S100A15 proteins are differentially expressed in human skin

A, Alignment of the predicted amino acid sequences of the human S100A7 (hS100A7, NP_002954) with the human S100A15 (hS100A15, NP_79669). Identical amino acid residues are indicated as blue boxes, and chemically similar amino acids are marked as grey boxes. Predicted EF-hand motifs for both proteins are marked above the sequences (variant S100-specific motif: amino acids 12–39, canonical EF-hand: amino acids 54–82). Indicated recombinant human S100 proteins (50 ng) and human keratinocyte lysates (20 ug), subjected to immunoblotting by incubation with monoclonal anti-hS100A7 or the affinity-purified polyclonal anti-hS100A15 antibody 3923. Solid arrows indicate the migration of the corresponding recombinant hS100A15 and hS100A7 monomers. Both antibodies detect the corresponding low and high molecular weight forms (asterisks) in keratinocyte lysate. The immunoreactive bands above the recombinant S100 monomers (open arrows) represent uncleaved recombinant MBP-hS100A7 and MBP-hS100A15 fusion proteins. *B*, Immunofluorescent staining of frozen sections of adult human skin stained for hS100A7 (green, upper left panel) and hS100A15 antibody (red, upper right panel). Co-staining of hS100A15 (red, lower panels) with Mart-1 (green, lower left panel) or smooth muscle actin (green, lower right panel). Full arrows indicate melanocytes, hollow arrows Langerhans cells and dendritic cells (lower left panel) or vascular endothelial cells (lower right panel). Nuclei were stained with DAPI (blue). Bar sizes: 50 μm. *C*, Chart summarizing expression and distribution of hS100A7/A15 in human skin based on immunostaining. *D*, Frozen sections of inflamed lesional psoriasis were stained for hS100A7 (green) and hS100A15 (red). Nuclei were stained with DAPI (blue). Bar size: 50 μm

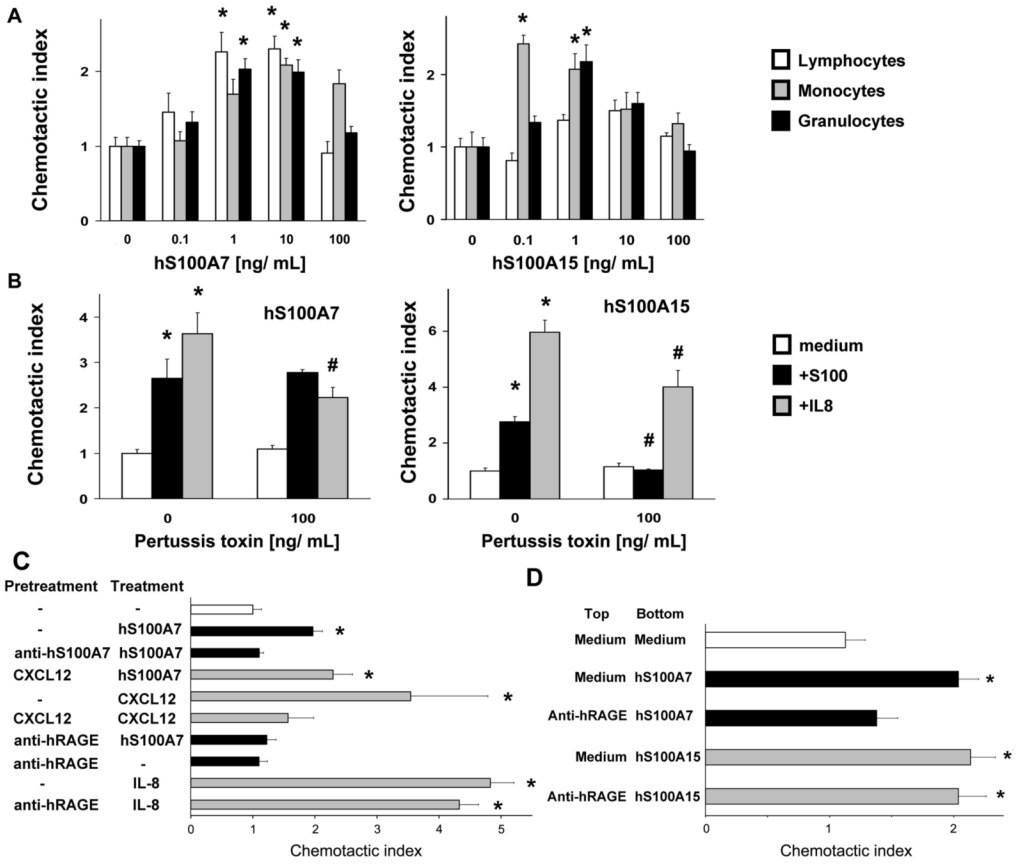

FIGURE 2. Both hS100A7 and hS100A15 are chemoattractants *in vitro*, but differ in cell targets and receptor activation

A, Chemotactic response of indicated leukocyte subsets from peripheral blood of human volunteers, evaluated using micro-Boyden chambers of specific pore size. Migrating cells on the filter surface of the lower chamber were stained for counting (1 ng/mL = 88.5 nM S100 protein). *B-D*, Chemotactic response of granulocytes (*B*) ± pertussis toxin pretreatment, *C*) pretreated (pretreatment) with medium, anti-hS100A7, CXCL12, anti-hRAGE before incubation (treatment) with medium, hS100A7, CXCL12, CXCL8/IL-8 as indicated, (*D*) with mediators placed in the top (medium, anti-hRAGE) or bottom (medium, hS100A7, hS100A15) chambers. *chemotactic index ≥ 2 of six samples from at least three individual volunteers, # statistically different compared to corresponding treatments ($P \leq 0.05$). Each bar represents mean, error bars indicate s.d.

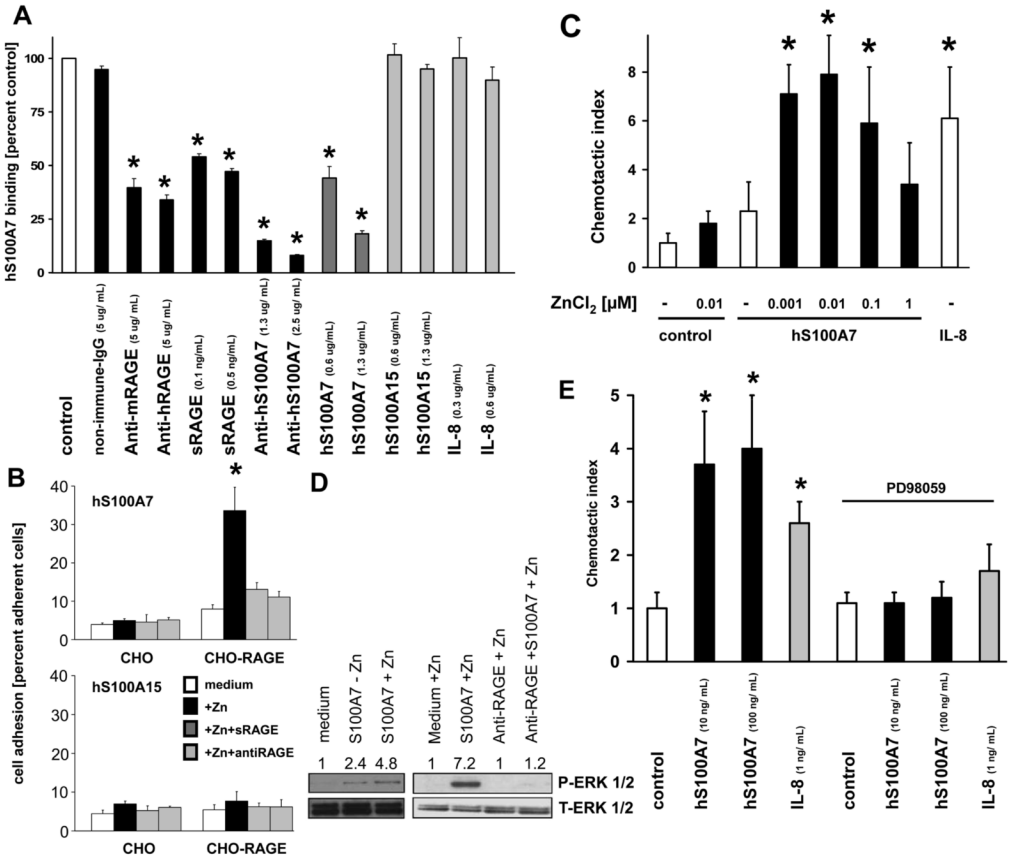

FIGURE 3. Binding, signaling and chemotaxis of hS100A7 is dependent on RAGE binding and zinc *in vitro*

A, Competitive ligand binding assay employing 200 ng of biotinylated hS100A7 binding to 100 ng murine soluble RAGE coated on polystyrene plates. Unlabeled competitors were added for 90 minutes at indicated concentrations and followed by streptavidine-alkaline phosphatase. Readout was performed as a luminescence signal (representative of two separate experiments, n=3, * $P \leq 0.05$. *B*, Cell adhesion assay employing control or murine RAGE-transfected Chinese hamster ovary cells to adhere to human S100A7 or human S100A15 in the absence and presence of zinc. Shaded bars show adhesion in the presence of soluble RAGE or anti-RAGE. (representative of three independent experiments, n=3, * $P \leq 0.05$. *C*, Chemotactic response of human peripheral granulocytes towards hS100A7 in the lower chamber in the absence or presence of increasing concentrations of zinc. (representative of three independent experiments, n=6, *$P \leq 0.05$. *D*, MAP kinase activation was determined in human peripheral blood neutrophils exposed to hS100A7 ± zinc chloride (15 nM). In some cases, cells were pre-treated with RAGE-neutralizing antibodies. Cell lysates were gel-separated and subjected to immunoblotting with indicated antibodies. Numbers above the lanes indicate relative phospho-ERK/total ERK increase. *E*, Chemotaxis of human peripheral blood neutrophils exposed to hS100A7 or IL-8/CXCL8 and pre-treated with ERK inhibitor PD98059 (10 μM) in the lower well of Boyden chambers. Migrating cells on the filter of lower chamber side were stained and counted, n=6, * chemotactic index ≥ 2. Each bar represents mean of six samples from at least three individual volunteers, error bars indicate s.d.

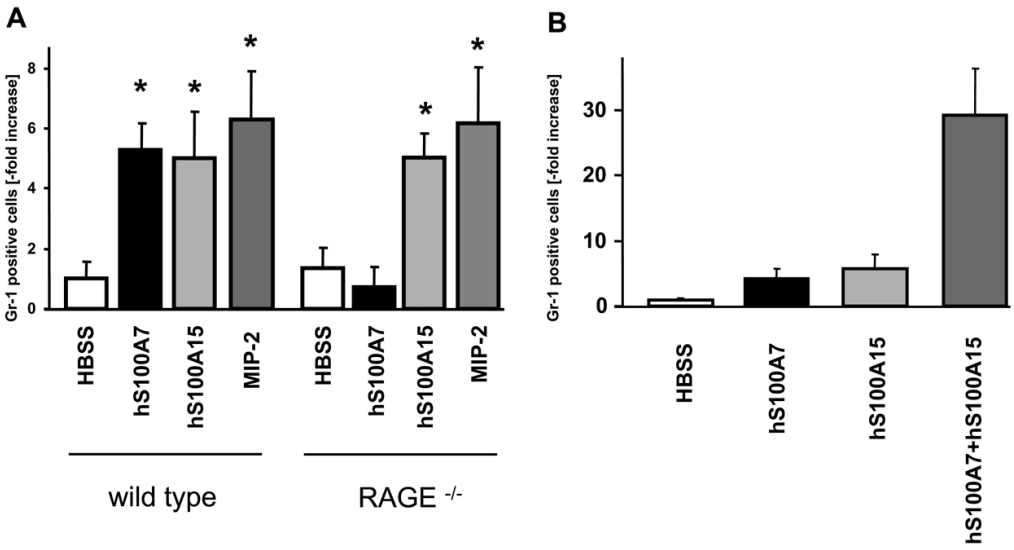

FIGURE 4. hS100A7 and hS100A15 act synergistically to induce inflamation *in vivo*, but differ in receptor activation

20 μg of recombinant hS100A7, hS100A15 or MIP-2 were injected intraperitoneally into C57/BL6 wild-type and RAGE−/− mice *A*) alone or *B*) premixed hS100A7 and hS100A15 (20 μg each) in combination. After four hours, cells attracted into the peritoneal fluid were counted and analyzed by flow cytometry using the granulocyte marker Gr-1. (representative of three separate experiments, each time point represents the mean value + s.d. from six mice, * $P \leq 0.05$).